Heterogeneous Interaction of H2O2 with TiO2 Surface under Dark and UV Light Irradiation Conditions

ARTICLE *in* THE JOURNAL OF PHYSICAL CHEMISTRY A · JULY 2012

Impact Factor: 2.69 · DOI: 10.1021/jp305366v · Source: PubMed

3 AUTHORS:

Manolis N Romanias
Ecole des Mines de Douai
25 PUBLICATIONS **99** CITATIONS
SEE PROFILE

Atallah El Zein
Université du Littoral Côte d'Opale (ULCO)
13 PUBLICATIONS **119** CITATIONS
SEE PROFILE

Yuri Bedjanian
CNRS Orleans Campus
67 PUBLICATIONS **853** CITATIONS
SEE PROFILE

THE JOURNAL OF PHYSICAL CHEMISTRY A

Article

pubs.acs.org/JPCA

Heterogeneous Interaction of H_2O_2 with TiO_2 Surface under Dark and UV Light Irradiation Conditions

Manolis N. Romanias,* Atallah El Zein, and Yuri Bedjanian

Institut de Combustion, Aérothermique, Réactivité et Environnement (ICARE), CNRS, 45071 Orléans Cedex 2, France

Supporting Information

ABSTRACT: The heterogeneous interaction of H_2O_2 with TiO_2 surface was investigated under dark conditions and in the presence of UV light using a low pressure flow tube reactor coupled with a quadrupole mass spectrometer. The uptake coefficients were measured as a function of the initial concentration of gaseous H_2O_2 ($[H_2O_2]_0$ = (0.17−120) × 10^{12} molecules cm^{-3}), irradiance intensity (J_{NO_2} = 0.002−0.012 s^{-1}), relative humidity (RH = 0.003−82%), and temperature (T = 275−320 K). Under dark conditions, a deactivation of TiO_2 surface upon exposure to H_2O_2 was observed, and only initial uptake coefficient of H_2O_2 was measured, given by the following expression: $\gamma_0(\text{dark}) = 4.1 \times 10^{-3}/(1 + \text{RH}^{0.65})$ (calculated using BET surface area, estimated conservative uncertainty of 30%) at T = 300 K. The steady-state uptake coefficient measured on UV irradiated TiO_2 surface, $\gamma_{ss}(\text{UV})$, was found to be independent of RH and showed a strong inverse dependence on $[H_2O_2]$ and linear dependence on photon flux. In addition, slight negative temperature dependence, $\gamma_{ss}(\text{UV}) = 7.2 \times 10^{-4} \exp[(460 \pm 80)/T]$, was observed in the temperature range (275−320) K (with $[H_2O_2] \approx 5 \times 10^{11}$ molecules cm^{-3} and J_{NO_2} = 0.012 s^{-1}). Experiments with NO addition into the reactive system provided indirect evidence for HO_2 radical formation upon H_2O_2 uptake, and the possible reaction mechanism is proposed. Finally, the atmospheric lifetime of H_2O_2 with respect to the heterogeneous loss on mineral dust was estimated (using the uptake data for TiO_2) to be in the range of hours during daytime, i.e., comparable to H_2O_2 photolysis lifetime (~1 day), which is the major removal process of hydrogen peroxide in the atmosphere. These data indicate a strong potential impact of H_2O_2 uptake on mineral aerosol on the HO_x chemistry in the troposphere.

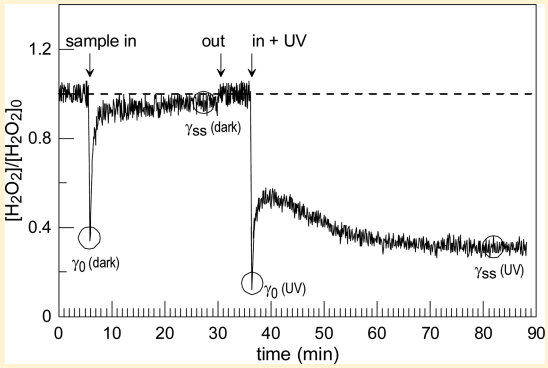

1. INTRODUCTION

According to recent estimations every year 1600 Tg of mineral dust is released in the atmosphere.[1] Although the primary sources of the dust particles are arid regions, due to the global air circulation aerosol particles undergoing long-range transportation to populated areas and influencing the air quality and public health.[2,3] The dust surfaces provide the seedbed for trace gas molecules adsorption-reaction and therefore are considered to play a key role in the transformation and environmental fate of many atmospheric species.[4,5] Titanium dioxide, TiO_2, is a component of atmospheric mineral dust aerosol particles, with mass mixing ratios ranging from 0.1% to 10%, depending on the location of the source.[3,6] Despite its relatively low abundance, TiO_2 may have an important impact on the reactivity of atmospheric aerosol due to its high photocatalytic efficiency. TiO_2 is an n-type semiconductor material with energy band gap 3.2 eV. When a photon with energy equal or higher to the energy gap of TiO_2 particles ($\lambda \leq 387$ nm) is absorbed, an electron (e^-) is promoted from the valence band to the conduction band leaving a hole (h^+) behind, initiating a series of oxidation−reduction reactions between TiO_2 particles and adsorbed donor and/or acceptor molecules.[7,8]

Hydrogen peroxide is an important atmospheric oxidant directly related to the HO_x radicals budget and chemistry in the troposphere.[9−11] H_2O_2 is a secondary photochemical product since it is produced by the self-reaction of HO_2 radicals

$$HO_2 + HO_2 \rightarrow H_2O_2 + O_2$$

while the two dominant removal pathways of H_2O_2 are photolysis and reaction with OH radicals

$$H_2O_2 + h\nu(\lambda \leq 360\ \text{nm}) \rightarrow 2OH$$

$$H_2O_2 + OH \rightarrow HO_2 + H_2O$$

Therefore, the atmospheric concentration of H_2O_2 is affected by the levels of chemical components such as NO_x, CO, CH_4, and nonmethane hydrocarbons. Moreover, meteorological parameters such as solar radiation, water vapor concentration, temperature, and pressure also influence gas phase hydrogen peroxide chemistry.[12,13] Typical mixing ratios of H_2O_2 in the troposphere lie between 0.5 and 5 ppbv, increasing up to 11.5 ppbv in the marine troposphere.[14,15] In addition, because of the high water solubility (Henry's law constant is ~10^5 M atm^{-1}), H_2O_2 is acting as an important oxidant of sulfur compounds in

Received: June 1, 2012
Revised: July 11, 2012
Published: July 17, 2012

   dx.doi.org/10.1021/jp305366v | J. Phys. Chem. A 2012, 116, 8191−8200

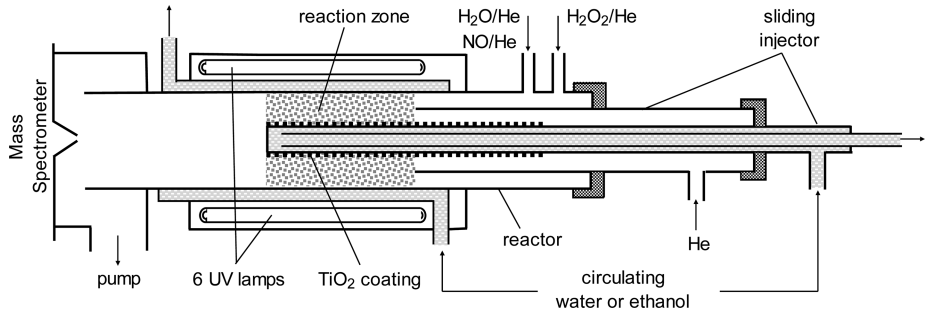

Figure 1. Diagram of the flow photoreactor.

the aqueous phase and may play a potentially important role in the formation of secondary organic aerosols.[9]

Recent studies have shown that the large discrepancies between observed and modeled H_2O_2 concentrations in a Sahara dust plume and in the Arctic spring troposphere can be reduced, after incorporating the heterogeneous uptake of H_2O_2 and HO_2 on aerosol surfaces, revealing a crucial role of these processes in the tropospheric photochemistry.[16,17] In this respect, a detailed quantitative understanding of the removal of atmospheric H_2O_2 by mineral dust aerosol is of importance for an accurate assessment of its lifetime and potential impact on the tropospheric chemistry of HO_x family, OH budget, and ozone balance. Available information on the kinetics of H_2O_2 interaction with mineral oxide surfaces is rather scarce and seems to be limited to a few studies,[18−21] realized under dark conditions.

The aim of the current study was to investigate the interaction of H_2O_2 with TiO_2 surface under dark and UV irradiation conditions. The uptake coefficients were measured as a function of initial concentration of H_2O_2 ($[H_2O_2]_0$ = (0.17−120) × 10^{12} molecules cm^{-3}), irradiation intensity, relative humidity (RH = 0.003−82%), and temperature (275−320 K) . To our knowledge, this is the first measurement of the uptake coefficient of H_2O_2 to TiO_2 surface in presence of light.

2. EXPERIMENTAL SECTION

2.1. Preparation of TiO_2 Surfaces. Solid TiO_2 films were deposited on the outer surface of a Pyrex tube (0.9 cm outer diameter) using TiO_2 (Sigma Aldrich, Aeroxide P25, (50 ± 15) m^2 g^{-1} surface area, ∼20 nm particle diameter) suspension in ethanol. Prior to film deposition, the Pyrex tube was treated with hydrofluoric acid and washed with distilled water and ethanol. Then, the tube was immersed into the suspension, withdrawn, and dried with a fan heater. Afterward, in order to eliminate the possible residual traces of ethanol, prior to uptake experiments, the freshly prepared TiO_2 samples were heated at (150−170) °C under pumping for 20−30 min. Finally, at the end of the adsorption experiment, the TiO_2 powder deposited on the glass tube was mechanically removed, and its mass was measured using a high accuracy mass balance. The uncertainty in the sample mass measurement ranged from a few to 30% (being higher for lowest masses).

2.2. Flow Tube−Mass Spectrometer Apparatus. The uptake experiments of H_2O_2 with TiO_2 surfaces were performed using a flow tube reactor (FT), employed in the laminar flow regime, and coupled with a modulated molecular beam quadrupole mass spectrometer (QMS) for the detection of the gas phase species. The FT/QMS technique has been used extensively in the past to measure the uptake of gas phase molecules with soot,[22−24] salt,[25,26] and mineral oxide surfaces.[27−29] Therefore, only a brief description of the experimental setup will be presented herein. The experimental setup consists of the gas preparation vacuum line, the flow tube reactor, and the differentially pumped stainless steel high-vacuum chamber that hosts the quadrupole mass spectrometer (Balzers, QMG 420). The gas phase molecules sampled from the flow reactor were modulated by a tuning-fork chopper (35 Hz), ionized through impact with high kinetic energy electrons (∼30 eV) emitted by the ion source of the mass spectrometer and detected using an electron multiplier. Subsequently, mass spectrometric signals were filtered and amplified with a lock-in amplifier and recorded for further analysis.

The flow tube reactor, which is shown in Figure 1, was used in a coaxial configuration. It consists of a Pyrex tube (40 cm length and 2.4 cm internal diameter) with a jacket for the thermostatted liquid circulation. The Pyrex tube with the deposited TiO_2 sample was introduced into the main reactor along its axis. This tube could be moved relative to the outer tube of the injector (Figure 1), allowing the variation of the TiO_2 sample length exposed to H_2O_2 and consequently the reaction time (t). Externally, the reactor was surrounded by 6 UV lamps (Sylvania BL350, 8 W) with a broad UV emission spectrum between 315−400 nm. The UV lamps were installed into an aluminum light-tight box covering the main reactor tube. Therefore, by switching on or off the lamps, we had the ability to perform kinetic measurements under UV irradiation or dark conditions, respectively. The irradiance intensity in the reactor was characterized by direct measurements of the NO_2 photolysis frequency, J_{NO2}, as a function of the number of lamps switched on. The values of J_{NO2} were found to be between 0.002 and 0.012 s^{-1} for 1 to 6 lamps switched on, respectively.[28]

2.3. Determination of Gas Phase Concentrations. The H_2O_2 vapors were delivered to the reactor by flowing 100 sccm He through the aqueous solution of H_2O_2 (60% wt H_2O_2/H_2O), stored in a glass bulb. H_2O_2 flow was then mixed with the total flow of ∼400 sccm of He (carrier gas) inside the reactor. The absolute calibration of H_2O_2 has been performed by injecting known amounts (0.5−10 μL) of the 60 wt % solution inside the flow tube reactor and recording the parent mass peak intensity of H_2O_2 at m/z = 34. The integrated area of the mass spectrometric signals corresponding to the known total number of H_2O_2 molecules injected into the reactor allowed the determination of the calibration factor. The H_2O vapors were introduced into the flow reactor by passing 100 sccm of He through thermostatted (20−30 °C) glass bubbler with deionized water. The concentrations of water were determined by calculating the H_2O flow rate from the total (H_2O + He) and H_2O vapor pressures in the bubbler and the measured flow rate of the He through the bubbler. The concentrations of other stable species (NO and NO_2) used in

dx.doi.org/10.1021/jp305366v | J. Phys. Chem. A 2012, 116, 8191−8200

this study were calculated from their flow rates measured by recording the pressure drop in calibrated volume storage flasks. NO and NO_2 were detected at their parent peaks, m/z = 30 and 46, respectively.

3. RESULTS

Typical uptake profiles of H_2O_2 on TiO_2 surfaces under dark and UV irradiation conditions are presented in Figure 2. The

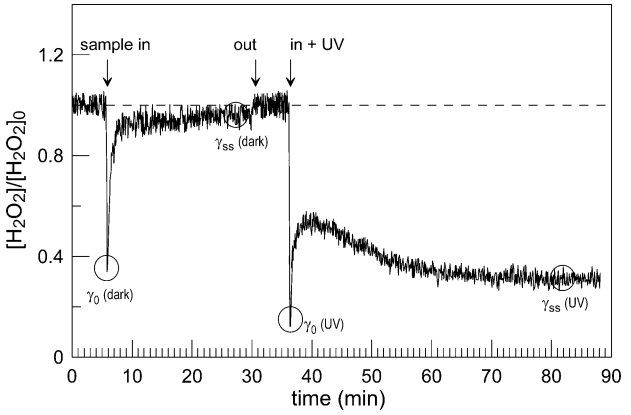

Figure 2. Typical uptake profiles of H_2O_2 on TiO_2 surface under dry conditions in the absence (dark conditions) and in presence of UV irradiation. The experiments have been performed at T = 300 K; P = 1 Torr with $[H_2O_2]_0 = 9 \times 10^{11}$ molecules cm^{-3}; and sample mass = 0.09 mg $cm^{-1} \times 10$ cm.

signal recorded during the first five minutes in Figure 2 corresponds to the initial concentration of H_2O_2 introduced into the reactor. Afterward, the glass tube with the deposited TiO_2 film is exposed to the gas flow (sample in), causing a rapid decrease of the MS signal due to H_2O_2 adsorption reaction with the mineral surface. Under dark conditions, the rapid initial drop (5 min) was followed by fast signal recovery almost to the initial pre-exposed level within the first 20 min, indicating the deactivation of the TiO_2 surface. Different behavior was observed under UV irradiation. The initial rapid decrease of the MS signal (in + UV, 36 min) was followed by a fast recovery (36–40 min), and subsequent gradual decrease with time up to the final stabilization after nearly 45 min of total exposure of the irradiated TiO_2 sample to H_2O_2 (87 min). This unusual uptake behavior can be attributed to a delayed photoactivation of the TiO_2 surface. Indeed, the initial part of the H_2O_2 profile observed under UV irradiation is similar to that under dark conditions; however, upon UV irradiation, the photocatalyst is gradually activated with time, enhancing H_2O_2 consumption. This type of kinetics was observed under dry conditions only. Under relatively high RH, where initial uptake of H_2O_2 under dark conditions is negligible compared with that in the presence of light, the initial fast drop of the H_2O_2 signal did not occur, and concentration profiles of H_2O_2 (under UV irradiation) represented a gradual decrease of $[H_2O_2]$ from initial to steady-state value. In the present study, we have measured the initial uptake coefficient of H_2O_2 under dark conditions (γ_0(dark)) and steady-state uptake coefficient on irradiated TiO_2 surface (γ_{ss}(UV)). The quasi steady-state uptake of H_2O_2 under dark conditions, being always at least an order of magnitude lower than the initial one, was found to decrease with exposure time. Consequently, it was not measured, and only the upper limit for γ_{ss}(dark) was determined, $\gamma_{ss}(\text{dark}) \leq 2 \times 10^{-5}$, which is valid under all experimental conditions of the study.

The uptake coefficient of H_2O_2 on TiO_2 surface was determined using the following expression:

$$\gamma = \frac{4k'_{kin}}{\omega}\frac{V}{S} \quad \text{(I)}$$

where k'_{kin} is the first order rate coefficient of H_2O_2 loss (s^{-1}) in the kinetic regime (see below), ω the average molecular speed (cm s^{-1}), V the volume of the reaction zone (cm^3), and S the surface area of the TiO_2 sample participating in the reaction (cm^2). Under certain experimental conditions, both ω and V are known parameters of the system; therefore, only k'_{kin} and S need to be determined experimentally.

3.1. Determination of k'_{kin}. The kinetics of H_2O_2 consumption in the heterogeneous reaction was explored in a set of experiments where different lengths of TiO_2 samples were exposed to the same initial concentration of H_2O_2. The results are shown in Figure S1 (Supporting Information). Solid lines represent exponential fits to the experimental points. The conclusion of these experiments was that heterogeneous loss of H_2O_2 could be described by a first order kinetics with the rate constant, k'_{obs}, defined by the following expression:

$$k'_{obs} = -\frac{d\ln([H_2O_2])}{dt} = \frac{\ln\left(\frac{I_0}{I(L)}\right)v}{L} \quad \text{(II)}$$

where I_0 and $I(L)$ are MS signal intensities corresponding to the initial concentration of H_2O_2 and that when in contact with the TiO_2 sample, respectively, v is the flow velocity in the reaction zone (cm s^{-1}) and L (cm) is the length of the TiO_2 sample exposed to H_2O_2.

The rate coefficient of H_2O_2 loss on TiO_2 surface in the kinetic regime, k'_{kin}, can be directly measured from a typical experiment only when the uptake of the gas molecules is not limited by their diffusion from volume toward the reactive surface. Under such conditions, which define the kinetic regime, no further analysis is required for the determination of k'_{kin}, and it can be directly determined using eq II ($k'_{kin} = k'_{obs}$). However, when an effective heterogeneous loss leads to an important local depletion of the gas phase molecules close to the surface, their diffusion from the volume of the reactor toward the surface becomes rate-limiting, and it should be included in the treatment of the experimental data. In this case, the approach based on the kinetic resistance additivity rule is usually used[30]

$$\frac{1}{k'_{obs}} = \frac{1}{k'_{kin}} + \frac{1}{k'_{dif}} \quad \text{(III)}$$

where k'_{obs} is the observed rate coefficient (s^{-1}), measured from the heterogeneous decay kinetics according to eq II, and k'_{kin} and k'_{dif} are the kinetic and diffusion limits of the rate coefficient, respectively. The rate constant k'_{dif} for our experimental configuration is given by the equation[31,32]

$$k'_{dif} = K^d(q)\frac{D}{R^2} \quad \text{(IV)}$$

where $K^d(q)$ is the dimensionless rate constant of radial diffusion, which is a function of ratio $q = r/R$; r is the external radius of the coated tube and R the internal radius of the main flow reactor. For our configuration, r = 0.45 cm and R = 1.2 cm,

dx.doi.org/10.1021/jp305366v | J. Phys. Chem. A 2012, 116, 8191–8200

q = 0.375, and $K^d(q)$ = 4.4.[32] By combining eqs III and IV we obtain

$$\frac{1}{k'_{obs}} = \frac{1}{k'_{kin}} + \frac{R^2}{K^d(q)D_0}P \qquad (V)$$

where D_0 (in Torr cm^2 s^{-1}) is the diffusion coefficient of H_2O_2 in He, which was the carrier gas, at 1 Torr pressure, and P is the total pressure in the reactor. We have carried out a series of experiments, where the rate of H_2O_2 loss on TiO_2 surface, k'_{obs}, was measured as a function of pressure in the reactor the former being varied in the range 1−10 Torr. The observed, relatively strong, pressure dependence of k'_{obs} is displayed in Figure 3. The experimental points are fitted with linear

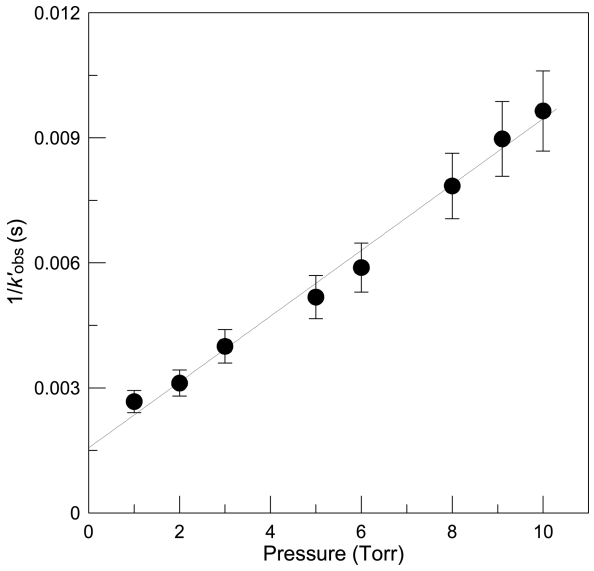

Figure 3. Reciprocal of the observed steady-state rate constant of H_2O_2 decay on irradiated (6 lamps on) TiO_2 surface as a function of the total pressure in the reactor: T = 300 K; P = 1−10 Torr; $[H_2O_2]_0$ = 5 × 10^{11} molecules cm^{-3}. The error bars correspond to estimated (nearly 10%) uncertainty on the measurements of k'_{obs}. The solid line is a linear fit of the experimental results according to eq V.

regression according to eq V. The intercept and the slope of the straight line provide the values of $1/k'_{kin}$ and $R^2/K^d(q)D_0$, respectively, that allows the determination of k'_{kin} (640 ± 160 s^{-1} (2σ) in this particular case) and the diffusion coefficient of H_2O_2 in He at 1 Torr total pressure and 300 K

$$D_0(\pm 2\sigma) = (415 \pm 35)\ \text{Torr cm}^2\ \text{s}^{-1}$$

It can be noted that this value for the diffusion coefficient of H_2O_2 in He is in good agreement with those measured for the polar diffusive analogue of H_2O_2 and HO_2 radical: $D_0(HO_2-He)$ = (430 ± 30)[33] and (405 ± 50) Torr cm^2 s^{-1}.[24] The determined diffusion coefficient was used through this study (assuming $T^{1.75}$-dependence of D_0 on temperature) to calculate k'_{kin} (via eq V). In the presence of water in the reactor, the diffusion coefficient of H_2O_2 was calculated using Blanc's empirical law. The experimental conditions for the measurements of the uptake coefficient were always chosen to minimize the diffusion corrections. However, the uptake coefficient of H_2O_2 on TiO_2 being rather high, the diffusion corrections applied to k'_{obs} ranged from a few percents up to nearly a factor of 2. The maximum corrections were applied to k'_{obs}(UV) data measured at highest RH where relatively high, up to 10 Torr, total pressure in the reactor was used to provide the appropriate partial pressure of water in the reactor.

3.2. Dependence on Sample Mass. In this series of experiments, the uptake of H_2O_2 was measured as a function of the mass of TiO_2 sample exposed to the H_2O_2 flow. The objective was to determine the TiO_2 surface area involved in the interaction with H_2O_2 molecules. The experiments were performed under UV irradiation at T = 300 K and dry conditions (RH = 2.5 × 10^{-3}). The obtained results are presented in Figure 4, where the uptake coefficient of H_2O_2,

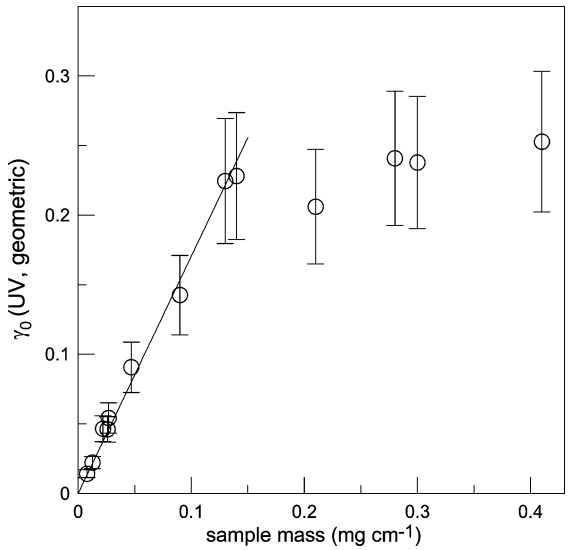

Figure 4. Initial uptake coefficient of H_2O_2 (calculated using geometric surface area) on irradiated TiO_2 surface as a function of TiO_2 sample mass (per 1 cm length of the support tube): 6 lamps on; dry conditions; T = 300 K; P = 1 Torr; $[H_2O_2]_0$ = 5 × 10^{11} molecules cm^{-3}; sample mass = 0.01−0.41 mg cm^{-1}.

calculated applying the geometric surface area of TiO_2 sample (γ_0(UV, geometric)), is shown as a function of the TiO_2 mass deposited per unity length of the support tube. Two different regimes can be observed in this graph corresponding to (a) linear dependence of the uptake coefficient on mass of TiO_2 sample for mass ≤ 0.13 mg cm^{-1} and (b) γ_0(UV, geometric) independent of the sample mass (saturation region) for mass > 0.13 mg cm^{-1}. In the linear regime, the entire surface area of the solid sample is considered to be accessible to H_2O_2, and consequently, the BET surface area should be used for the determination of the true uptake coefficient. On the contrary, at higher thickness of TiO_2 films (saturation regime), the H_2O_2 molecules do not reach the lowermost layers of the coating: consequently, only a limited part of the TiO_2 sample is involved in the heterogeneous reaction, and the measured (geometric) uptake coefficient is independent of the sample mass. In the present study, all the uptake measurements were carried out using TiO_2 coating thickness corresponding to the linear regime, and BET surface area was used to calculate the uptake coefficients under dark and UV light conditions. The linear dependence in Figure 4 provides the following value of the initial uptake coefficient of H_2O_2 on irradiated TiO_2 surface (6 lamps on) under dry conditions and T = 300 K: γ_0(UV) = (9.6 ± 2.9) × 10^{-3}, where uncertainty includes a statistical one, and those on BET surface area and on the measurements of k'_{kin}. It must be noted that the values obtained for the uptake

dx.doi.org/10.1021/jp305366v | J. Phys. Chem. A 2012, 116, 8191−8200

coefficients in the present study using BET surface area should be considered as lower limits.

3.3. Dependence on Initial Concentration of H_2O_2. The dependence of the uptake coefficient on initial concentration of H_2O_2 in the gas phase was studied for $[H_2O_2]_0$ varied between 1.7×10^{11} and 1.2×10^{14} molecules cm^{-3}. Experiments have been performed at T = 300 K, dry conditions, and 1 Torr total pressure in the reactor. The results obtained for γ_0(UV) and γ_{ss}(UV) are displayed in Figure 5. The

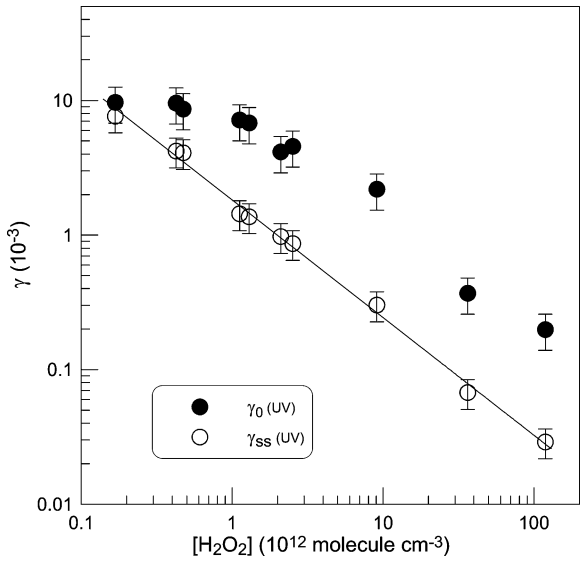

Figure 5. Uptake coefficient as a function of the initial H_2O_2 concentration: T = 300 K; P = 1 Torr. The error bars reflect the estimated uncertainties of 25 and 30% on determination of γ_{ss} and γ_0, respectively.

initial uptake coefficient was independent of H_2O_2 concentration for $[H_2O_2]_0 \leq 1 \times 10^{12}$ molecules cm^{-3}; however, at $[H_2O_2]_0$ exceeding this value, inverse dependence of γ_0(UV) on H_2O_2 concentration was observed. Generally, initial uptake (in case of first order kinetics) is not expected to be dependent on the gas phase concentration of the reactant since, at the initial stage of the surface exposure, the active sites on the surface are not depleted or blocked and are all available for the heterogeneous reaction. The observed decrease of γ_0(UV) at higher $[H_2O_2]_0$ was most likely due to limited time resolution of our detecting system leading to a cutting of the sharp initial H_2O_2 adsorption peaks. Regarding the steady-state uptake coefficient in presence of UV light, a strong inverse dependence of γ_{ss}(UV) on $[H_2O_2]_0$ was observed in the whole H_2O_2 concentration range according to the following empirical expression:

$$\gamma_{ss}(\mathrm{UV}) = ((1.8 \pm 0.2) \times 10^{-3})([H_2O_2]_0)^{-(0.88\pm0.05)}$$

where concentration of H_2O_2 is in 10^{12} molecules cm^{-3} units and quoted uncertainties are 2σ statistical ones. The inverse dependence of the steady-state uptake on concentration of H_2O_2 may be due to the surface saturation by the adsorbed precursor and/or depletion of photoproduced intermediates. With the purpose of comparison, the measurements of the uptake coefficient under different experimental conditions presented below were carried out with the initial concentration of H_2O_2 fixed at nearly 5×10^{11} molecules cm^{-3}. This value was the result of a compromise between the need to work with low concentrations relevant to the atmosphere and H_2O_2 detection limit.

3.4. Dependence on Irradiation Intensity. The photocatalytic efficiency of a semiconductor, such as TiO_2, depends on the irradiance intensity of the incident light that activates the material. The objective of the present series of experiments was to measure the steady-state uptake coefficient of H_2O_2 as a function of the irradiance intensity. TiO_2 samples were exposed to the same initial concentration, $[H_2O_2]_0 \approx 5 \times 10^{11}$ molecules cm^{-3}, at T = 300 K and dry conditions, and the uptake coefficients were measured as a function of the number of UV lamps switched on (0 to 6 lamps). The results of these experiments (Figure 6) showed a linear relationship between

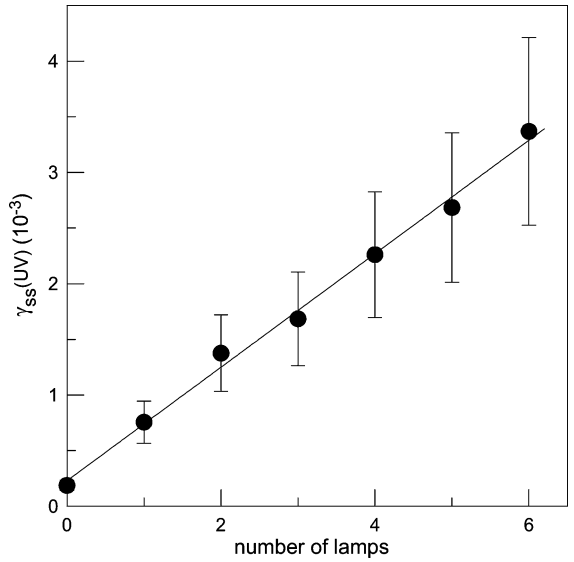

Figure 6. Steady-state uptake coefficient as a function of the irradiation intensity (number of lamps switched on): T = 300 K; P = 1 Torr; $[H_2O_2]_0 \approx 5 \times 10^{11}$ molecules cm^{-3}. The error bars show the estimated 25% uncertainties on determination of γ_{ss}.

γ_{ss}(UV) and irradiance intensity pointing to the photocatalytic nature of the heterogeneous reaction. The intercept of the straight line in Figure 6 agrees well with the value of γ(dark) = $(1.9 \pm 0.5) \times 10^{-4}$ measured under dark conditions (prior to the experiments with irradiated surface) with TiO_2 sample exposed to H_2O_2 during 5 min. This value is much higher compared with those of γ_{ss}(dark) measured at longer exposure times. It can be noted that the UV irradiance level used in the present experiments was close to that under real atmospheric conditions. In fact, the range of values of J_{NO2} between 0.002 and 0.012 s^{-1} for 1 to 6 lamps switched on in our reactor overlaps with the values of J_{NO2} measured in the atmosphere under cloud and clear sky conditions.[34−36]

3.5. Dependence on Relative Humidity. The uptake coefficients of H_2O_2 were investigated as a function of relative humidity, and the results are displayed in Figure 7. The experiments have been performed at T = 275 K in order to achieve high levels of RH, relevant to those in the atmosphere, inside our low pressure flow reactor.

Under dark conditions, only the initial uptake coefficient, γ_0(dark), was measured since the TiO_2 surface was almost fully deactivated, and γ_{ss}(dark) values at elevated RH were too low to be measured in our flow tube system. As it can be seen in Figure 7 (filled circles), for the relative humidity in the range

dx.doi.org/10.1021/jp305366v | J. Phys. Chem. A 2012, 116, 8191−8200

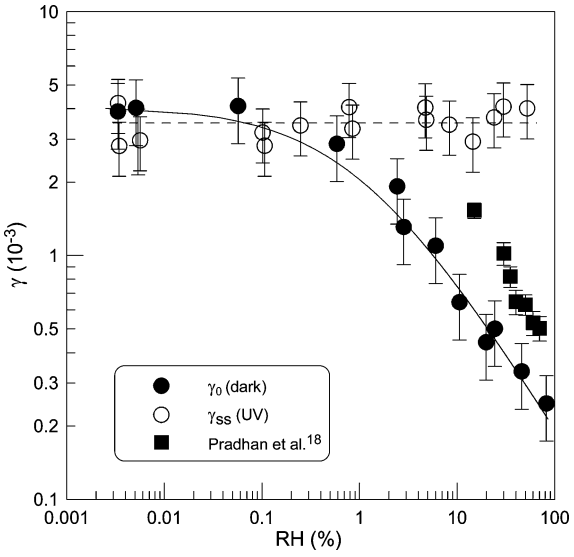

Figure 7. Uptake coefficients measured as a function of relative humidity: T = 275 K; pressure range P = 1−10 Torr; $[H_2O_2]_0 \approx 5 \times 10^{11}$ molecules cm^{-3}. Filled circles, initial uptake coefficient under dark conditions; open circles, steady-state uptake coefficient under UV irradiation (6 lamps on); filled squares, data from Pradhan et al.[18] measured under dark conditions.

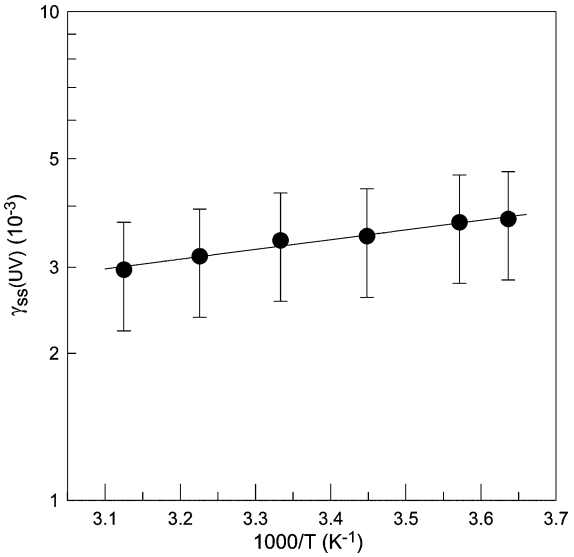

Figure 8. Temperature dependence of the steady-state uptake coefficient of H_2O_2 on irradiated TiO_2 surface (6 lamps on): P = 1 Torr; T = 275−320 K; RH = 0.3%; $[H_2O_2]_0 \approx 5 \times 10^{11}$ molecules cm^{-3}.

(0.003−0.1)% the independent RH value of around 4×10^{-3} was measured for γ_0(dark). However, a further increase of RH resulted in a decrease of the uptake coefficient down to the value of ~2.5×10^{-4} at 82% RH. The solid line in Figure 7 is a power fit of the experimental data according to the following expression:

$$\gamma_0(\text{dark}) = 4.1 \times 10^{-3}/(1 + \text{RH}^{0.65})$$

This is an empirical equation without any physical meaning, describing our results (with estimated conservative uncertainty of 30%) in the whole RH range used.

The steady-state uptake coefficient measured under UV irradiation conditions, γ_{ss}(UV), was found to be independent of the relative humidity in the entire range of RH used in these experiments, (0.003−52)%. The dashed line in Figure 7 corresponds to the mean value of the steady-state coefficient:

$$\gamma_{ss}(\text{UV}) = (3.5 \pm 0.9) \times 10^{-3}$$

It should be recalled that all the uptake coefficients were calculated using BET surface area of the TiO_2 samples. The inverse dependence of the uptake coefficient on RH observed under dark conditions can be attributed to competition between water and hydrogen peroxide molecules for the available active sites on the surface. Under UV irradiation (γ_{ss}(UV) independent of RH), the effect of the blocking of surface active sites by water is probably compensated by the role of water as a source of OH radicals.

3.6. Temperature Dependence. Temperature dependence of the uptake coefficient was measured for γ_{ss}(UV). The experiments have been performed in the temperature range (275−320) K with initial concentration of $H_2O_2 \approx 5 \times 10^{11}$ molecules cm^{-3} at a fixed relative humidity (RH ≈ 0.3%). The results are presented in Figure 8. As one can note, the uptake coefficient was found to decrease slightly with increasing temperature. The solid line in Figure 8 represents an exponential fit to the experimental data and provides the following Arrhenius expression for γ_{ss}(UV):

$$\gamma_{ss}(\text{UV}) = ((7.2 \pm 1.9) \times 10^{-4}) \exp[(460 \pm 80)/T]$$

at T = 275−320 K (uncertainties are 2σ statistical ones).

3.7. Addition of NO. The photocatalytic decomposition of H_2O_2 on metal oxide surfaces has been extensively studied in the past, mainly in the liquid phase. In the published data, different mechanisms have been proposed depending on the experimental observations of each study.[37−40] However, in all the proposed mechanisms, OH and HO_2 radicals appear as intermediate products of this interaction. Therefore, one can expect that these reactive species can also be present in products of the gas−solid interaction of TiO_2 surfaces with gaseous H_2O_2 molecules. In order to obtain qualitative information on the reaction products, we have carried out a series of experiments investigating the H_2O_2 interaction with irradiated TiO_2 surface in the presence of NO. The initial idea was to probe the TiO_2 surface and/or the gas phase for HO_2 radicals by their reaction with NO with subsequent detection of NO_2 formed

$$HO_2 + NO \rightarrow OH + NO_2$$

In the gas phase, the rate coefficient of this reaction is 8.8×10^{-12} cm^3 molecule^{-1} s^{-1} at T = 298 K.[41]

Typical experiments consisted of the introduction of the TiO_2 sample into the irradiated reactor (under dry conditions and T = 300 K) in contact with H_2O_2 and NO and monitoring of the yield of NO_2 under varied experimental conditions (concentrations of NO and H_2O_2, irradiation intensity). The NO_2 yield was determined as a ratio of the NO_2 concentration formed to the concentration of H_2O_2 consumed: NO_2 yield = $\Delta[NO_2]/\Delta[H_2O_2]$. The NO_2 yield was observed to be dependent on exposure time, being lower at the initial stage of the reaction and progressively increasing with time to its maximum steady value. Possible reasons for the delayed formation of NO_2 observed during the first phase of the heterogeneous reaction will be discussed later. It should be

dx.doi.org/10.1021/jp305366v | J. Phys. Chem. A 2012, 116, 8191−8200

pointed out that all the measurements presented below were conducted under stabilized NO_2 yield conditions, that is, upon reaching its maximum.

Figure 9 summarizes the results of a set of experiments, where the NO_2 yield was investigated as a function of the

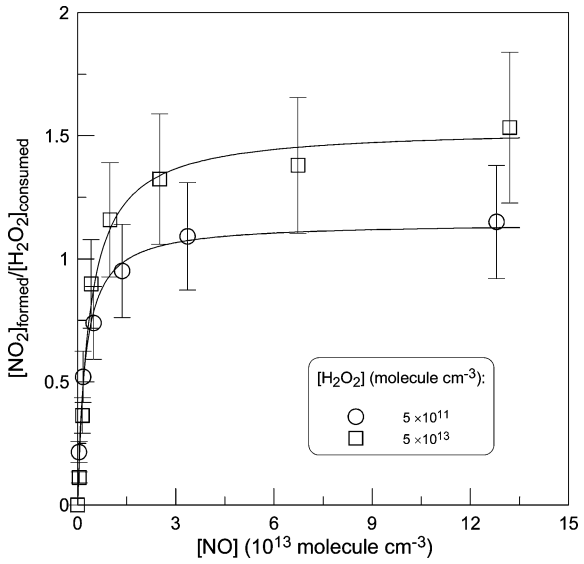

Figure 9. H_2O_2 + TiO_2 in the presence of NO. NO_2 yield as a function of NO concentration: T = 300 K; dry conditions; the error bars reflect estimated 20% uncertainty on the measurements of the NO_2 yield.

concentration of NO. It is observed that the product yield increases with increasing [NO] and levels off at its maximum value at [NO] $\geq 5 \times 10^{13}$ molecules cm^{-3}. The observed dependence of NO_2 yield on NO concentration could be expected, being most probably due to the competition of the reaction of HO_2 with NO, with other HO_2 loss processes not leading to NO_2 formation. Another observation is that the maximum NO_2 yield depends (although not strongly) on the concentration of H_2O_2, being nearly 1.1 and 1.5 for $[H_2O_2] = 5 \times 10^{11}$ and 5×10^{13} molecules cm^{-3}, respectively. This dependence was confirmed in the experiments where NO_2 yield was measured as a function of H_2O_2 concentration (Figure S2, Supporting Information). The observed yields of NO_2 were found to be independent of the UV irradiation intensity (from 1 to 6 lamps switched on). In order to verify the nitrogen mass balance, we have measured the dependence of the concentration of NO_2 formed on the concentration of NO consumed (Figure 10). The straight line in Figure 10 represents a linear through origin fit to the experimental data and shows a nearly unity slope, indicating a stoichiometric conversion of NO to NO_2.

With the reactive system being rather complex, we have carried out a series of blank experiments to ensure that detected NO_2 resulted from the NO reaction with products of H_2O_2 decomposition. It was verified that, under the experimental conditions of the study, neither NO uptake to TiO_2 surface (fresh sample or treated with H_2O_2 prior to exposure to NO) nor NO_2 formation were occurring in the absence of H_2O_2 in the reactor (with and without the addition of water).

In specific experiments, we attempted to test the gas flow leaving the reaction zone (defined by the length of the TiO_2 coating exposed to H_2O_2) for the presence of OH and/or HO_2 radicals. TiO_2 surface was exposed to the gas H_2O_2 flow, while

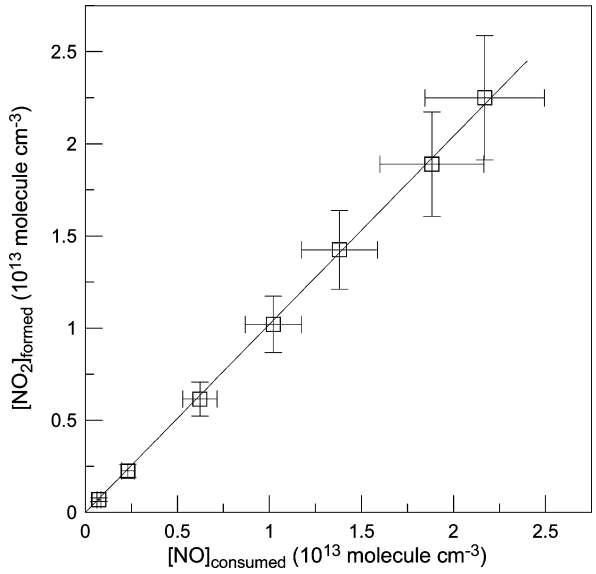

Figure 10. H_2O_2 + TiO_2 in the presence of NO. Concentration of NO_2 formed as function of consumed concentration of NO: T = 300 K; dry conditions; the error bars correspond to 15% uncertainty on the measurements of the species concentrations.

NO was introduced into the reactor through the interior of the tube with TiO_2 coating. In this configuration, NO is not in contact with the reactive surface and is mixed with the reactants and products of the heterogeneous reaction immediately at the exit of the reaction zone. Under these conditions, we did not observe any formation of NO_2 indicating that HO_2 radicals are mainly localized on the TiO_2 surface and/or are rapidly taken up by the surface even if they are released into the gas phase. Similar experiments were carried out with the addition of Br_2 instead of NO. The purpose was to probe the gas flow leaving the reaction zone for OH radicals by their conversion to stable HOBr species via reaction with Br_2[42]

$$OH + Br_2 \rightarrow HOBr + Br$$

As is the case with HO_2 radicals, we found no trace of OH radicals in the gas phase. An upper limit of $\sim 10^{10}$ molecules cm^{-3} can be estimated for the concentrations of both HO_2 and OH in the gas flow leaving the reaction zone.

4. DISCUSSION

4.1. Comparison with Previous Studies. To our knowledge, this is the first measurement of the uptake coefficient of H_2O_2 on mineral oxide surface under UV irradiation. However, the present results can be compared with available data measured under dark conditions. As far as we know, there is only one published study concerning the measurements of the H_2O_2 uptake to TiO_2 surfaces by Pradhan et al.[18] Using an aerosol flow tube reactor coupled with a chemical ionization mass spectrometer for the detection of H_2O_2 molecules, the authors investigated the impact of the relative humidity on the uptake coefficient of H_2O_2, in the range of 15−70% RH, at room temperature under dark conditions. The uptake coefficient of H_2O_2 was found to decrease by a factor of nearly 2 as the RH was increased from 15% to 40%: $\gamma = (1.53 \pm 0.11) \times 10^{-3}$ and $(6.47 \pm 0.74) \times 10^{-4}$, respectively. For RH > 40%, the uptake coefficient of H_2O_2 was considered to be invariable within the experimental uncertainty. Considering the method used by Pradhan et al.[18]

dx.doi.org/10.1021/jp305366v | J. Phys. Chem. A 2012, 116, 8191−8200

(continuous flow of the aerosol/H_2O_2 mixture, i.e., rather short aerosol to H_2O_2 exposure times), the values of γ measured in their study (and included in Figure 7, filled squares) correspond to the initial uptake and can be compared with the data for γ_0(dark) measured in the present study (Figure 7, filled circles). We have found γ_0(dark) to be independent of relative humidity under lowest RH of the study (<0.1%), while in the RH range between 0.1 and 82%, a substantial decrease of γ_0(dark) was observed. As one can see in Figure 7, the results obtained for γ_0(dark) in both studies show similar trends with regard to RH dependence; however, the absolute values of the uptake coefficients differ by a factor of about 2. Nevertheless, in our opinion, the agreement between the results of two studies obtained by different methods (aerosol versus bulk samples) can be considered as very reasonable, especially if one considers that our values of γ calculated with BET surface area represents a lower limit and those of Pradhan et al.[18] an upper limit of the uptake coefficient (because the aerosol surface area was calculated from the measured aerosol mobility diameter assuming that the particles are spherical). The systematic error induced by the nonspherical shape of mineral dust particles can be as high as a factor of 1.5 to 2.[19]

In another study, using a similar experimental approach, Pradhan et al.[19] have measured the uptake coefficients of hydrogen peroxide on authentic Gobi and Saharan dust aerosol particles. The range of absolute values of γ observed with both Gobi and Saharan dusts ($(3.3–9.4) \times 10^{-4}$, the corresponding values for Saharan dust being systematically higher) in RH range between 15 and 70% was not very different from that measured with TiO_2 surface. However, in contrast to the TiO_2 surface, a positive correlation of the uptake coefficient with RH has been observed. Wang et al.[20] using Knudsen cell reactor measured the initial uptake coefficients of H_2O_2 on α-Al_2O_3, MgO, Fe_2O_3, and SiO_2 under dry conditions: γ_0(dark) = 1.0×10^{-4}, 1.7×10^{-4}, 9.7×10^{-5}, and 5.2×10^{-5}, respectively. Zhao et al.[21] investigated the heterogeneous interaction of H_2O_2 with two major components of mineral dust aerosol, SiO_2 and α-Al_2O_3 particles. The uptake coefficients were found to decrease with relative humidity from 1.5×10^{-8} and 1.2×10^{-7} at 2% RH to 0.6×10^{-8} and 0.8×10^{-7} at 76% RH for SiO_2 and α-Al_2O_3, respectively. These values of γ, corresponding to a steady-state uptake, are nearly 3 orders of magnitude lower than those measured in the present study (for TiO_2 surface) and by Pradhan et al. for the initial uptake of H_2O_2 on TiO_2[18] and Gobi and Saharan dust particles.[19]

4.2. Reaction Mechanism. On the basis of the available literature data, a set of reactions probably involved in the H_2O_2 reactive uptake to TiO_2 surface under UV irradiation can be proposed. Initially, the absorbed UV light activates the surface material promoting an electron to the conduction band and leaving a hole in the valence band

$$TiO_2 + h\nu \rightarrow h^+ + e^- \quad (1)$$

The electrons and holes formed lead to the reduction and oxidation reactions, respectively

$$h^+ + H_2O \rightarrow OH + H^+ \quad (2)$$

$$h^+ + H_2O_2 \rightarrow HO_2 + H^+ \quad (3)$$

$$e^- + H_2O_2 \rightarrow OH + OH^- \quad (4)$$

$$h^+ + OH^- \rightarrow OH \quad (5)$$

The primary reaction products, OH and HO_2 radicals, can be further involved in the secondary reactions

$$OH + H_2O_2 \rightarrow HO_2 + H_2O \quad (6)$$

$$OH + HO_2 \rightarrow H_2O + O_2 \quad (7)$$

$$OH + OH \rightarrow H_2O_2 \quad (8a)$$

$$OH + OH \rightarrow H_2O + O \quad (8b)$$

$$HO_2 + HO_2 \rightarrow H_2O_2 + O_2 \quad (9)$$

The addition of NO into the reactive system initiates a series of reactions involving the nitrogen oxide species

$$HO_2 + NO \rightarrow NO_2 + OH \quad (10)$$

$$NO_2 + OH \rightarrow HNO_3 \quad (11)$$

$$NO_2 + e^- \rightarrow NO_2^- \quad (12)$$

$$NO_2^- + H^+ \rightarrow HONO \quad (13)$$

$$NO_2^- + h\nu \rightarrow NO + O^- \quad (14)$$

According to this reaction scheme and considering that H_2O_2 and HO_2 are consumed exclusively via reactions 3 and 10, the maximum yield of NO_2 formed in the $TiO_2 + H_2O_2$ reaction in the presence of NO cannot exceed one (one NO_2 molecule formed per one H_2O_2 consumed). However, this is in contradiction with the experimental observation of NO_2 yields up to 1.5. In addition, it should be noted that the experiments were carried out in the absence of oxygen in the gas flow, so that the possible significant formation of HO_2 (and consequently, of NO_2) in reaction 15 can be excluded

$$H^+ + O_2^- \rightarrow HO_2 \quad (15)$$

It is clear that the additional NO_2 must be sought in the surface reactions initiated by OH radicals. In fact, OH radicals can react with NO to form HONO[43,44]

$$OH + NO \rightarrow HONO \quad (16)$$

Indeed, the presence of HONO on the surface was confirmed in the test experiment where the TiO_2 sample treated with H_2O_2 + NO mixture was first pumped in the flow of helium and then heated (up to 150 °C). Upon heating, a release of gas phase species at m/z = 47 was observed and attributed to HONO. In our recent study,[29] we have shown that HONO readily reacts with TiO_2 surface even under dark conditions forming NO_2 and NO in the gas phase with nearly 60 and 40% yields, respectively. On the irradiated TiO_2 surface, we have observed similarly close to 50% yields for both products (not yet published data)

$$HONO + TiO_2 \rightarrow NO + \text{products} \quad (17a)$$

$$HONO + TiO_2 \rightarrow NO_2 + \text{products} \quad (17b)$$

The maximum yield of NO_2 can be calculated in the frame of this mechanism (considering the equal branching ratio of 0.5 for reactions 17a and 17b) for two scenarios. For the first one, where H_2O_2 reacts with TiO_2 surface exclusively via reaction 3, the maximum yield of NO_2 formed in the sequence of reactions 3, 10, 16, 17a, and 17b is 1.5. In this scenario, where H_2O_2 reacts with TiO_2 surface via reaction 4, the NO_2 yield calculated involving reactions 4, 5, 16, 17a, and 17b may not exceed 1. These considerations combined with experimental observations

seem to point out that reaction 3 is the dominant pathway of H_2O_2 interaction with TiO_2 surface under UV irradiation. This conclusion is in line with the results of the recent study of Yi et al.,[45] where HO_2 radicals released into the gas phase upon H_2O_2 removal by UV irradiated TiO_2 surface were directly detected using cavity ring down spectroscopy. Regarding the present study, it should be noted that the conclusion of predominant formation of HO_2 in H_2O_2 + TiO_2 reaction under UV irradiation is based on the equal yield of 0.5 for NO_2 and NO in reactions 17a and 17b, which was measured in the absence of H_2O_2 in a reactive system. In the presence of H_2O_2, the distribution of the products of HONO + TiO_2 reaction may be different. The impact of H_2O_2 on the products of the HONO interaction with TiO_2 surface may be also responsible for the observed dependence of the NO_2 yield on concentration of H_2O_2 (Figure S2, Supporting Information), which is difficult to explain in the frame of the proposed mechanism.

As noted in the Results, a lower yield of gaseous NO_2 was observed during the first minutes of TiO_2 exposure to H_2O_2 + NO mixture. This delayed formation of NO_2 could be due to limited desorption of the product from the TiO_2 surface and/or to initial uptake of NO_2[27,28] leading to formation of the intermediate species such as HONO and HNO_3 on the surface with subsequent release of NO_2 under UV irradiation. Experimental observations seem to support these assumptions. First, the uptake of NO_2 (present as a trace impurity in NO) was really observed at the initial stage of the reaction. Second, as mentioned above, the presence of HONO on the surface was confirmed in the thermal desorption experiment of the reacted TiO_2 samples. In another test experiment, we have observed an emission of NO_2 upon UV irradiation in a flow of helium of the TiO_2 sample that had previously been treated with H_2O_2 + NO.

It is clear that the proposed mechanism remains speculative. The main gap is associated with the reactivity of TiO_2 surface toward different species (in our case, HONO and NO_2) in the presence of H_2O_2. H_2O_2 is a source of the active species on the surface (HO_2 and, perhaps, OH radicals) and can dramatically change the surface reactivity. The striking example of that is the interaction of NO with the TiO_2 surface: we have observed that NO readily reacts with the TiO_2 surface in the presence of H_2O_2, while no NO uptake was observed under similar experimental conditions in the absence of H_2O_2. These arguments seem to raise the question of the applicability for atmospheric modeling of the uptake data measured in laboratory for pure gases and emphasize the need to study the heterogeneous processes (at least, on photoactive surfaces) using multicomponent systems.

4.3. Atmospheric Implications. The atmospheric lifetime, τ_{het}, of H_2O_2 molecules due to the heterogeneous loss onto an aerosol surface can be calculated as

$$\tau_{het} = \frac{1}{k'_{het}} = \frac{4}{\gamma \omega A} \quad \text{(VI)}$$

where k'_{het} is the first order rate coefficient of the heterogeneous loss of H_2O_2 (s^{-1}), γ is the uptake coefficient, ω is the mean molecular velocity (cm s^{-1}), and A the aerosol surface area density (cm^2 cm^{-3}). Pradhan et al.,[18] using the uptake coefficient value measured at 35% RH (γ = 8.20 × 10^{-4}), aerosol surface area density 1.5 × 10^{-6} cm^2 cm^{-3}, calculated the lifetime of H_2O_2 under dark conditions to be ~21 h. This estimation should be considered as a lower limit of the H_2O_2 lifetime since the authors used the initial uptake coefficient measured after 15 s exposure of the TiO_2 samples to H_2O_2. The steady-state uptake coefficients are more relevant for the atmospheric modeling of the reactivity of the aged mineral dust particles. In the present study, we have estimated that the steady-state uptake of H_2O_2 to TiO_2 surface under dark conditions is at least by an order of magnitude lower than the initial one. In fact, the steady state uptake may be even lower as indicated by the study of Zhao et al.,[21] where $\gamma_{ss} \approx 10^{-7}$ was measured for α-Al_2O_3 particles.

The experimental data obtained in the present study for H_2O_2 uptake on UV irradiated TiO_2 surface can be applied to assess the potential role of H_2O_2 loss on mineral aerosols during daytime. Using the independent relative humidity values of γ_{ss}(UV) measured with 1 (J_{NO2} = 0.002 s^{-1}, cloud sky conditions) and 6 UV lamps switched on (J_{NO2} = 0.012 s^{-1}, clear sky conditions),[36] γ_{ss}(1 L) = 7.5 × 10^{-4} and γ_{ss}(6 L) = 3.5 × 10^{-3}, the lifetime of H_2O_2 with respect to heterogeneous loss is estimated to be approximately 22 and 5 h, respectively. These numbers should be compared to the photolysis lifetime of H_2O_2 of ~1 day. Furthermore, the calculated lifetimes of H_2O_2 may be even shorter given the observed dependence of the steady-state uptake coefficient on H_2O_2 concentration, which was higher in the present study compared with those in the atmosphere. The above considerations show that the uptake of H_2O_2 on mineral aerosol during daytime may have a significant impact on the chemistry of HO_x family, concentration of OH and, consequently, on O_3 budget in the troposphere. However, it should be noted that, in the above estimations, we have used the uptake data measured on titanium oxide, which is the most reactive photocatalytic component of mineral dust. It is clear that additional experimental studies on the interaction of H_2O_2 with real mineral aerosols and their different constituents in the presence of irradiation are needed in order to better assess the atmospheric impact of the H_2O_2 uptake. This is a subject of current investigations in our group.

■ ASSOCIATED CONTENT

Supporting Information

Examples of kinetics of H_2O_2 consumption on irradiated TiO_2 surface (Figure S1); NO_2 yield from H_2O_2 + TiO_2 reaction in presence of NO as a function of initial concentration of H_2O_2 (Figure S2). This material is available free of charge via the Internet at http://pubs.acs.org.

■ AUTHOR INFORMATION

Corresponding Author

*Tel: +33 238255474. Fax: +33 238696004. E-mail: manolis.romanias@cnrs-orleans.fr.

Notes

The authors declare no competing financial interest.

■ ACKNOWLEDGMENTS

This study was supported by ANR from Photodust grant. A.E.Z. is very grateful to région Centre for financing his Ph.D. grant.

■ REFERENCES

(1) Andreae, M. O.; Rosenfeld, D. *Earth Sci. Rev.* **2008**, *89*, 13.
(2) Kanatani, K. T.; Ito, I.; Al-Delaimy, W. K.; Adachi, Y.; Mathews, W. C.; Ramsdell, J. W. *Am. J. Respir. Crit. Care Med.* **2010**, *182*, 1475.
(3) Usher, C. R.; Michel, A. E.; Grassian, V. H. *Chem. Rev.* **2003**, *103*, 4883.

(4) Dentener, F. J.; Carmichael, G. R.; Zhang, Y.; Lelieveld, J.; Crutzen, P. J. *J. Geophys. Res.* **1996**, *101*, 22869.
(5) Kolb, C. E.; Cox, R. A.; Abbatt, J. P. D.; Ammann, M.; Davis, E. J.; Donaldson, D. J.; Garrett, B. C.; George, C.; Griffiths, P. T.; Hanson, D. R.; Kulmala, M.; McFiggans, G.; Pöschl, U.; Riipinen, I.; Rossi, M. J.; Rudich, Y.; Wagner, P. E.; Winkler, P. M.; Worsnop, D. R.; O' Dowd, C. D. *Atmos. Chem. Phys.* **2010**, *10*, 10561.
(6) Karagulian, F.; Santschi, C.; Rossi, M. J. *Atmos. Chem. Phys.* **2006**, *6*, 1373.
(7) Herrmann, J. M. *Top. Catal.* **2005**, *34*, 49.
(8) Linsebigler, A. L.; Lu, G.; Yates, J. T. *Chem. Rev.* **1995**, *95*, 735.
(9) Hua, W.; Chen, Z. M.; Jie, C. Y.; Kondo, Y.; Hofzumahaus, A.; Takegawa, N.; Chang, C. C.; Lu, K. D.; Miyazaki, Y.; Kita, K.; Wang, H. L.; Zhang, Y. H.; Hu, M. *Atmos. Chem. Phys.* **2008**, *8*, 6755.
(10) Reeves, C. E.; Penkett, S. A. *Chem. Rev.* **2003**, *103*, 5199.
(11) von Kuhlmann, R.; Lawrence, M. G.; Crutzen, P. J.; Rasch, P. J. *J. Geophys. Res.* **2003**, *108*, 4729.
(12) Kleinman, L. I. *J. Geophys. Res.* **1991**, *96*, 20721.
(13) Logan, J. A.; Prather, M. J.; Wofsy, S. C.; McElroy, M. B. *J. Geophys. Res.* **1981**, *86*, 7210.
(14) Jacob, P.; Klockow, D. *J. Atmos. Chem.* **1992**, *15*, 353.
(15) O'Sullivan, D. W.; Heikes, B. G.; Lee, M.; Chang, W.; Gregory, G. L.; Blake, D. R.; Sachse, G. W. *J. Geophys. Res.* **1999**, *104*, 5635.
(16) De Reus, M.; Fischer, H.; Sander, R.; Gros, V.; Kormann, R.; Salisbury, G.; Van Dingenen, R.; Williams, J.; Zöllner, M.; Lelieveld, J. *Atmos. Chem. Phys.* **2005**, *5*, 1787.
(17) Mao, J.; Jacob, D. J.; Evans, M. J.; Olson, J. R.; Ren, X.; Brune, W. H.; Clair, J. M. S.; Crounse, J. D.; Spencer, K. M.; Beaver, M. R.; Wennberg, P. O.; Cubison, M. J.; Jimenez, J. L.; Fried, A.; Weibring, P.; Walega, J. G.; Hall, S. R.; Weinheimer, A. J.; Cohen, R. C.; Chen, G.; Crawford, J. H.; McNaughton, C.; Clarke, A. D.; Jaeglé, L.; Fisher, J. A.; Yantosca, R. M.; Le Sager, P.; Carouge, C. *Atmos. Chem. Phys.* **2010**, *10*, 5823.
(18) Pradhan, M.; Kalberer, M.; Griffiths, P. T.; Braban, C. F.; Pope, F. D.; Cox, R. A.; Lambert, R. M. *Environ. Sci. Technol.* **2010**, *44*, 1360.
(19) Pradhan, M.; Kyriakou, G.; Archibald, A. T.; Papageorgiou, A. C.; Kalberer, M.; Lambert, R. M. *Atmos. Chem. Phys.* **2010**, *10*, 7127.
(20) Wang, W.-G.; Ge, M.-F.; Sun, Q. *Chin. J. Chem. Phys.* **2011**, *24*, 515.
(21) Zhao, Y.; Chen, Z.; Shen, X.; Zhang, X. *Environ. Sci. Technol.* **2011**, *45*, 3317.
(22) Lelièvre, S.; Bedjanian, Y.; Laverdet, G.; Le Bras, G. *J. Phys. Chem. A* **2004**, *108*, 10807.
(23) Lelièvre, S.; Bedjanian, Y.; Pouvesle, N.; Delfau, J. L.; Vovelle, C.; Le Bras, G. *Phys. Chem. Chem. Phys.* **2004**, *6*, 1181.
(24) Bedjanian, Y.; Lelièvre, S.; Le Bras, G. *Phys. Chem. Chem. Phys.* **2005**, *7*, 334.
(25) Bedjanian, Y.; Loukhovitskaya, E. *J. Atmos. Chem.* **2009**, *63*, 97.
(26) Loukhovitskaya, E.; Bedjanian, Y.; Morozov, I.; Le Bras, G. *Phys. Chem. Chem. Phys.* **2009**, *11*, 7896.
(27) Bedjanian, Y.; El Zein, A. *J. Phys. Chem. A* **2012**, *116*, 1758.
(28) El Zein, A.; Bedjanian, Y. *Atmos. Chem. Phys.* **2012**, *12*, 1013.
(29) El Zein, A.; Bedjanian, Y. *J. Phys. Chem. A* **2012**, *116*, 3665.
(30) Frank-Kamenetskii, D. A. *Diffusion and Heat Transfer in Chemical Kinetics*; Plenum Press: New York, 1969.
(31) Gershenzon, Y. M.; Grigorieva, V. M.; Zasypkin, A. Y.; Remorov, R. G. Theory of Radial Diffusion and First Order Wall Reaction in Movable and Immovable Media. *Proceedings of the 13th International Symposium on Gas Kinetics*, Dublin, Ireland, 1994.
(32) Gershenzon, Y. M.; Grigorieva, V. M.; Ivanov, A. V.; Remorov, R. G. *Faraday Discuss.* **1995**, *100*, 83.
(33) Ivanov, A. V.; Trakhtenberg, S.; Bertram, A. K.; Gershenzon, Y. M.; Molina, M. J. *J. Phys. Chem. A* **2007**, *111*, 1632.
(34) Barnard, J. C.; Chapman, E. G.; Fast, J. D.; Schmelzer, J. R.; Slusser, J. R.; Shetter, R. E. *Atmos. Environ.* **2004**, *38*, 3393.
(35) Castro, T.; Rouiz-Squarez, G. L.; Gay, C. *Atmosfera* **1995**, *8*, 137.
(36) Kraus, A.; Hofzumahaus, A. *J. Atmos. Chem.* **1998**, *31*, 161.
(37) Li, X.; Chen, C.; Zhao, J. *Langmuir* **2001**, *17*, 4118.
(38) Walling, C.; Cleary, M. *Int. J. Chem. Kinet.* **1977**, *9*, 595.
(39) Walling, C.; Weil, T. *Int. J. Chem. Kinet.* **1974**, *6*, 507.
(40) Weiss, J. The Free Radical Mechanism in the Reactions of Hydrogen Peroxide. In *Advances in Catalysis*; Frankenburg, W. G., Komarewsky, V. I., Rideal, E. K., Eds.; Academic Press: New York, 1952; Vol. *4*; p 343.
(41) Atkinson, R.; Baulch, D. L.; Cox, R. A.; Crowley, J. N.; Hampson, R. F.; Hynes, R. G.; Jenkin, M. E.; Rossi, M. J.; Troe, J. *Atmos. Chem. Phys.* **2004**, *4*, 1461.
(42) Bedjanian, Y.; Le Bras, G.; Poulet, G. *Int. J. Chem. Kinet.* **1999**, *31*, 698.
(43) Devahasdin, S.; Fan, C., Jr; Li, K.; Chen, D. H. *J. Photochem. Photobiol., A* **2003**, *156*, 161.
(44) Folli, A.; Campbell, S. B.; Anderson, J. A.; Macphee, D. E. *J. Photochem. Photobiol., A* **2011**, *220*, 85.
(45) Yi, J.; Bahrini, C.; Schoemaecker, C.; Fittschen, C.; Choi, W. *J. Phys. Chem. C* **2012**, *116*, 10090.